# AADE-17-NTCE-21

# Sealing Pressure Prediction Model for Lost Circulation Treatments Based on Experimental Investigations

M. Alsaba, Australian College of Kuwait; M. Aldushaishi, Texas A&M International University; M. Jeennakorn, Missouri University of Science and Technology; R. Nygaard, Oklahoma State University; A. Saasen, University of Stavanger, and O. Nes, Aker BP ASA



## Abstract

Lost circulation events are one of the major contributors towards drilling-related non-productive time (NPT). Lost circulation materials (LCMs) are often applied as a remedial action to alleviate drilling fluid losses into fractured formations. In normal overbalanced drilling operations and when designing lost circulation treatments, it is important that the formed seal within the fractures maintain at least the minimum overbalance pressure without breaking. Predicting the sealing pressure of LCMs treatments, which is defined as the maximum pressure at which the formed seal breaks and fluid losses resumes, is crucial for an effective fracture sealing. This paper presents a linear model for sealing pressure prediction.

A statistical analysis was conducted on a data set, which was developed from a previous experimental investigation, to understand the relationship between different parameters and the sealing pressure of LCM treatments. The investigated parameters include fracture width, fluid density, LCM type/blend, base fluid, and particle size distribution (PSD).

The statistical analysis showed that the sealing pressure is highly dependent on the fracture width, fluid density, and PSD. A predictive linear fit model, which could be used as a useful tool to design LCM treatment prior to field application, was developed. The developed model correlated well with the collected data and resulted in an overall model accuracy of 80%.

Knowing the dominant parameters affecting the sealing pressure will help in designing LCMs treatments that are capable of sealing expected fracture widths as well as maintaining high differential pressures and thus, effectively mitigating fluid losses as soon as they occur.

## Introduction

Lost circulation events are considered to be one of the challenging problems to be prevented or mitigated where approximately 1.8 million bbls of drilling fluids are lost per year (Marinescu, 2014). This number explains the operational challenges caused by lost circulation. In addition, lost circulation events could delay further drilling and thus contributing towards increased cost of drilling operations as a result of non-productive time (NPT).

Proper remedial actions, as per a pre-designed contingency plans or decision trees (Savari and Whitfill, 2016), are often taken to mitigate or stop the losses once they occur depending on the loss severity. However, these contingencies plans neglect the need for the experimental evaluation of the most effective LCM blend on the rig site (Savari and Whitfill, 2016).

To verify the effectiveness of designed treatments, laboratory evaluation is a crucial step prior to field application. Different testing methods are used to evaluate the performance of LCM treatments, based on the fluid loss volume at a constant pressure, such as the particle plugging apparatus (PPA) or the high-pressure-high-temperature (HPHT) fluid loss in conjunction with slotted/tapered discs or ceramic discs (Whitfill 2008; Kumar et al. 2011; Kumar and Savari 2011).

Other testing equipment has been developed to evaluate the sealing efficiency of LCM treatments in sealing permeable/impermeable fractured formations (Hettema et al. 2007; Sanders et al. 2008; Van Oort et al. 2009; Kaageson-Loe et al. 2009). Both particle size distribution (PSD) and total LCM concentration were found to have a significant effect on the sealing efficiency. It was also concluded that the fluid loss volume is not a good parameter to measure the sealing efficiency of LCM treatments.

PSD is often used as the designing parameter for LCM treatments where different models such as Abrams median particle-size rule (Abrams, 1977), ideal packing theory (IPT) (Andreasen and Anderson, 1930), and Vickers method (Vickers et al. 2006) are used to optimize PSD.

The effect of other LCM properties such as crushing resistance, resiliency, and aspect ratio on the overall performance of LCM blends were evaluated by Kumar et al. (2010). It was concluded that higher crushing resistance and resiliency are desirable for both controlling fluid losses and wellbore strengthening applications.

In normal overbalanced drilling operations (i.e. drilling fluid pressure higher than formation pressure), a minimum static overbalance pressure of 150-300 psi is required to prevent formation fluid influx (Jahn et al. 2008; Rehm et al. 2012; The Drilling Manual, 2015). Therefore, when designing LCM treatments, it is important to ensure that the selected LCM blend is able to seal fractures effectively and stop losses. In addition, the formed seal within the fracture should withstand at least the minimum overbalance pressure without failing.

The main objective of this paper is to introduce the sealing pressure prediction model, which was developed based on a large data collected from experimental evaluation of different LCM blends used to seal different fracture widths at different fluid types and densities. The model can be used as a tool to evaluate the performance of the selected LCM treatment from the contingency plan without the need for extra experimental evaluation.

## Previous Experimental Investigation

The sealing pressure of LCM treatments was previously (Alsaba, 2015) measured using a high-pressure LCM testing apparatus. The sealing pressure is defined here as the maximum pressure at which the formed seal breaks and fluid loss resumes. **Figure 1** shows a schematic of the experimental setup, where a plastic accumulator (1) used to transfer the drilling fluids to the metal accumulator (2) prior to pressurizing the fluids containing LCM treatments inside the testing cell (3) through the tapered discs (4) using an Isco™ pump (DX100) (5) to provide injection pressure, which was connected to a computer to record pressure versus time.

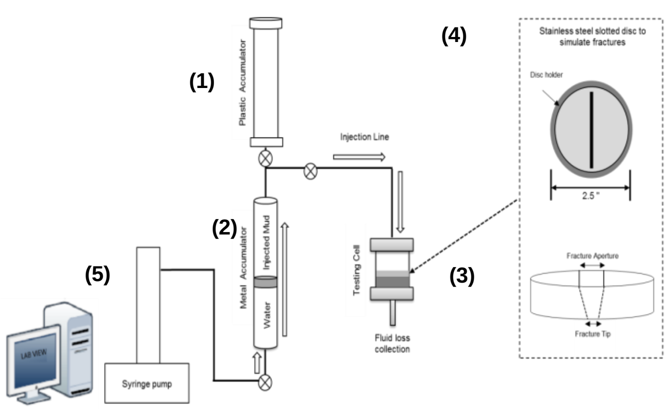


Figure 1. Schematic of the High Pressure Testing Apparatus

The effects of varying LCM type, formulation, concentration, fracture width, particle size distribution, base fluid, and density were studied with respect to differential pressure. The main objectives were to establish a better understanding of how these parameters could affect the sealing efficiency (in terms of pressure) of LCMs and identify their limitations in sealing fractures.

High-pressure tests were conducted on different LCM treatment formulations containing conventional LCMs such as graphite (G), sized calcium carbonate (SCC), nut shells (NS), and cellulosic fiber (CF) (Detailed formulation can be found in Alsaba, 2015) to evaluate their sealing efficiency at different fracture width varying between 1000 – 3000 microns. The LCM treatments were tested in both water-based mud (WBM) and oil-based mud (OBM) at different fluid densities ranging between 8.6 lb/gal and up to 16.5 lb/gal. The concentrations and the PSD of the LCM blends, which was measure using dry sieve analysis, used in this study are shown in **Table 1**.

Table 1. Summary of the Particle Size Distribution Analysis for the Different LCM Blends

| LCM Blend | Total Conc. (ppb) | Particle Size Distribution (microns) | | | | |
|---|---|---|---|---|---|---|
| | | D10 | D25 | D50 | D75 | D90 |
| G # 1 | 15 | 60 | 85 | 320 | 800 | 1300 |
| G # 1 | 50 | 60 | 95 | 340 | 800 | 1300 |
| NS # 1 | 15 | 180 | 400 | 1000 | 1600 | 2000 |
| NS # 1 | 50 | 180 | 400 | 1000 | 1600 | 2400 |
| SCC # 3 | 50 | 250 | 360 | 680 | 950 | 1200 |
| CF # 1 | 15 | 90 | 140 | 220 | 700 | 1400 |
| CF # 1 | 50 | 90 | 150 | 220 | 800 | 1400 |
| G & SCC # 1 | 30 | 80 | 100 | 460 | 900 | 1300 |
| G & SCC # 1 | 80 | 80 | 120 | 480 | 900 | 1300 |
| G & SCC # 3 | 105 | 65 | 90 | 420 | 1100 | 1400 |
| G & SCC # 4 | 105 | 60 | 150 | 500 | 700 | 900 |
| G & SCC # 5 | 105 | 90 | 400 | 700 | 1200 | 1400 |
| G & SCC # 6 | 105 | 100 | 500 | 900 | 1250 | 1400 |
| G & SCC # 7 | 105 | 170 | 650 | 1300 | 1900 | 2600 |
| G & SCC # 8 | 105 | 100 | 250 | 1000 | 1800 | 2400 |
| G & SCC # 9 | 105 | 300 | 800 | 1400 | 1800 | 2200 |
| G & NS # 1 | 20 | 65 | 180 | 500 | 1300 | 1900 |
| G & NS # 1 | 40 | 80 | 180 | 580 | 1400 | 2000 |

**NOTE: Graphite (G) Nutshells (NS) Sized Calcium Carbonate (SCC) Cellulosic Fiber (CF)**

## Statistical Methods

Statistical analysis of the LCM sealing pressure results for 75 high-pressure tests was performed to define the parameters with the highest effect on the sealing pressure.

A statistical analysis was conducted using JMP™ statistical analysis software to understand the relationship between the different investigated parameters such as fracture width, LCM type/blend, base fluid, and PSD on the performance of LCM in terms of the sealing pressure.

First, a regression analysis was conducted by performing a multiple linear regression analysis to model a relationship between 9 explanatory variables and the sealing pressure response. The 9 variables used are fracture width, LCM type/blend, base fluid, fluid density, and the five D-values obtained from PSD analysis; D10, D25, D50, D75, and D90.

The probability test (F-test) was performed to test the influence of each parameter on sealing pressure. The F-test provides a P-value, where the P-value is basically a statistical probability that the predicted value (in this case the F-value) is similar or very different from the measured value, assuming a true null hypothesis ($H_0$) that proposes no influence of a specific variable on the sealing pressure (Montgomery, 2001). With a confidence interval of 95% and type I error ($\alpha$) of 0.05, P-values less than 0.05 suggests rejecting the null hypothesis ($H_0$) and accepting an alternative hypothesis ($H_1$). The alternative hypothesis suggests that the sealing pressure is influenced by a specific variable. The F-test is calculated based on the variance of the data as:

$$F = \frac{S_1^2}{S_2^2} \quad (1)$$

Where $S_1^2$ is the variance of the first sample and $S_2^2$ is the variance of the second sample. The variance can be defined as the average squared difference from the mean.

Leverage plots for general linear hypothesis, introduced by Sall (1990), were plotted for each of the 9 variables (predictors) to show their contribution to the predicted sealing pressure. The Effect Leverage plot is used to characterize the hypothesis by plotting points where the distance between each point to the fit line shows the unconstrained residual while the distance to the x-axis shows the constrained residual by the hypothesis. The constrained sealing pressure for each parameter under the hypothesis can be written as:

$$b_0 = b - (X'X)^{-1}L'\lambda \quad (2)$$

Where b is the least square, $(X'X)$ is the inverse matrix (the transpose of the matrix data being D-values and other parameter, used to enforce orthogonality), and λ is the Lagrangian multiplier for the hypothesis constraint (L). The residual constrained by the hypothesis ($r_0$) is:

$$r_0 = r + X(X'X)^{-1}L'\lambda \quad (3)$$

Where the Lagrangian multiplier is defined as:

$$\lambda = (L(X'X)^{-1}L')^{-1}Lb \quad (4)$$

The residuals unconstrained by the hypothesis (r) are the least squares residuals defined as:

$$r = \acute{y} - Xb \quad (5)$$

The Leverage plot is constructed by plotting $v_x$ on the x-axis (Eq. 6) versus $v_y$ on the y-axis (Eq. 7). $v_x$ values represents the difference in the residuals caused by the hypothesis, which is the distance from the model fit line to the x-axis while $v_y$ values are $v_x$ plus the unconstrained residuals.

$$v_x = X(X'X)^{-1}L'\lambda \quad (6)$$

$$v_y = r + v_x \quad (7)$$

The sealing pressure residuals are regressed on all predictors except for the variable of interest while the x-residuals (variable of interest) are regressed on all other predictors in the model. The mean of the sealing pressure, without the effect of variable of interest, is plotted as well as a least square fit line and confidence interval for easier interpretation of the results. The upper and lower confidence interval could be plotted using Eq. 8 and Eq. 9, respectively. The least squares fit line slope is a measure of how the tested variable affects the sealing pressure i.e. a non-zero slope implies that the tested variable will affect the sealing pressure (Sall, 1990).

$$Upper\ (x) = xb + t_{\alpha/2}s\sqrt{x(X'X)^{-1}x'} \quad (8)$$

$$Lower\ (x) = xb - t_{\alpha/2}s\sqrt{x(X'X)^{-1}x'} \quad (9)$$

Where x = [1 *x*] is the 2-vector of regressors.

### *Statistical Analysis Results*

**Figures 2 - 10** show the Effect Leverage plots for each parameter with the resulting P value. The blue dashed line represents the mean sealing pressure, the solid red line represents the fitted model, and the dashed red line represents the confidence interval (5% confidence level). If the mean sealing pressure is inside the confidence interval envelope the parameter does not have any significant effect on sealing pressure. If the confidence interval crosses the mean pressure at a high angle, it has a significant contribution to sealing pressure.

**Figure 2** shows the effect of fracture width in the sealing pressure. The effect of fracture width is very significant since the confidence interval curves crossed the mean pressure with a high slope. The P-value of 0.0003 also indicates that the fracture width influenced the predicted sealing pressure. The effect of fluid density (**Figure 3**) was also pronounced since confidence curve crossed the horizontal line with a P-value that is less than 0.05 suggesting a good correlation.

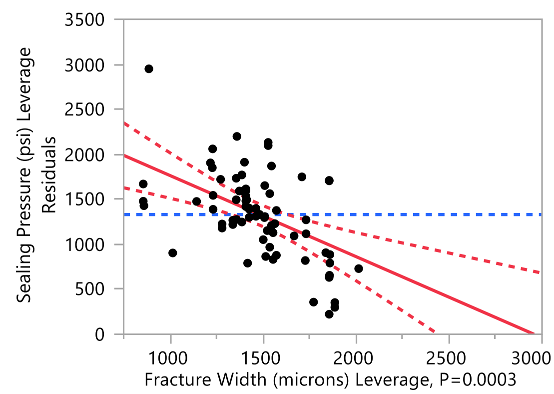


Figure 2. Leverage Plot Showing the Effect of Fracture Width on Sealing Pressure

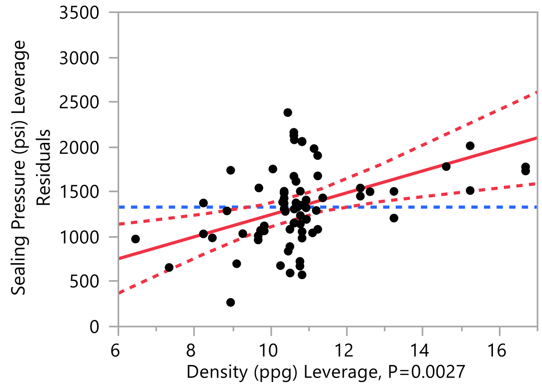


Figure 3. Leverage Plot Showing the Effect of Density on Sealing Pressure

The effect of D90 was the third significant parameter to affect the prediction of sealing pressure. The Effect of D90 can be clearly seen (**Figure 4**) with a P-value that is slightly larger than 0.05. The variation in LCM blends showed also a clear effect with P-value 0.1147 (**Figure 5**).

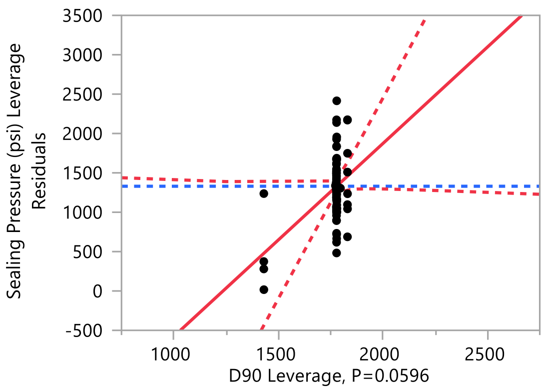


Figure 4. Leverage Plot Showing the Effect of D90 on Sealing Pressure

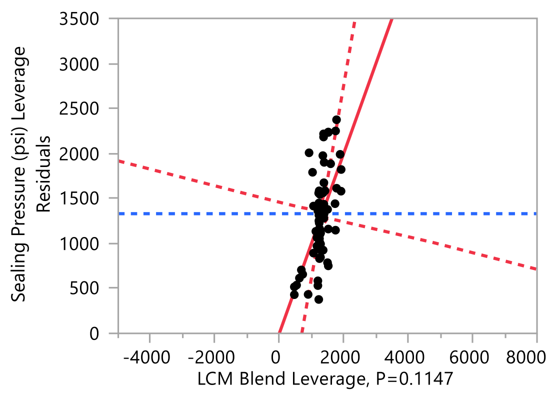


Figure 5. Leverage Plot Showing the Effect of LCM Blend on Sealing Pressure

The Effect Leverage plots (**Figures 6 – 10**) for D75, base fluid, D25, D50, and D10, respectively shows less effect on the sealing pressure with P-values ranging between 0.2863 and 0.9817. However, the less significance of these parameters might be due to the outliers in the analyzed data set.

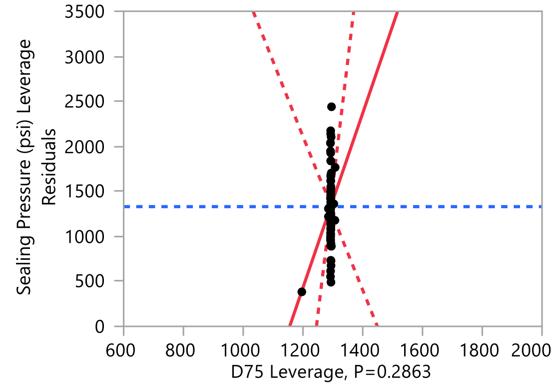


Figure 6. Leverage Plot Showing the Effect of D75 on Sealing Pressure

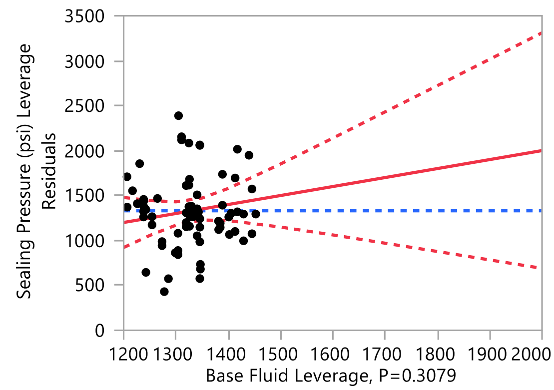


Figure 7. Leverage Plot Showing the Effect of Base Fluid on Sealing Pressure

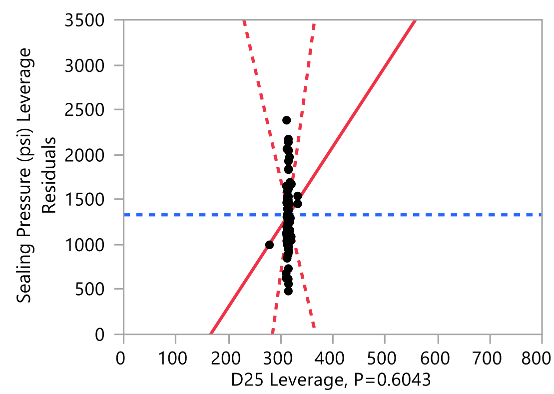


Figure 8. Leverage Plot Showing the Effect of D25 on Sealing Pressure

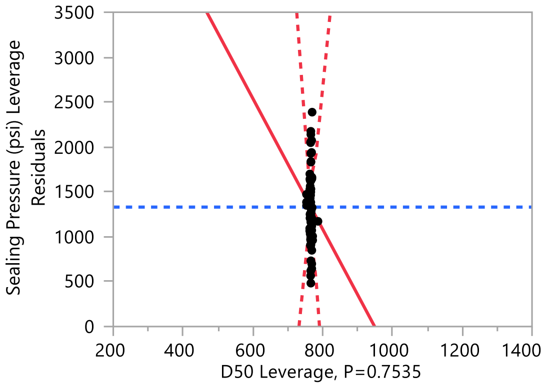


Figure 9. Leverage Plot Showing the Effect of D50 on Sealing Pressure

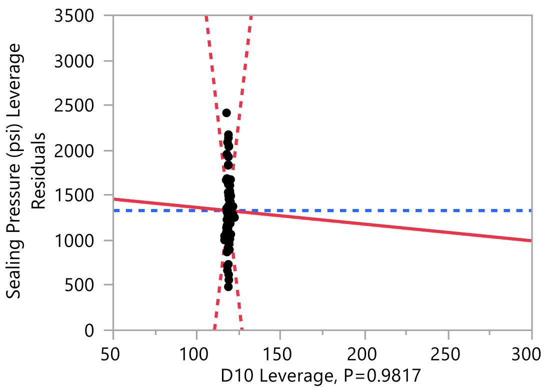


Figure 10. Leverage Plot Showing the Effect of D10 on Sealing Pressure

The predictive linear fit model shown in **Figure 11** shows a good correlation with an $R^2$ of 80% and a P-value less than 0.05. The residual plot (Figure 12) showed the data being randomly distributed around x-axis, verifying that a linear model was appropriate for the collected data. **Table 2** summarizes the P-values for the different variables as well as the model fit $R^2$.

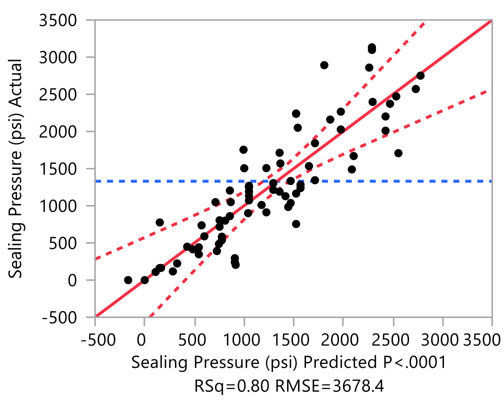


Figure 11. Leverage Plot Showing the Actual Sealing Pressure versus the Predicted Sealing Pressure using the fit model

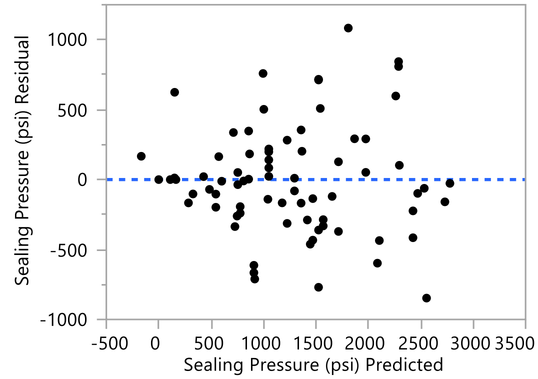


Figure 12. Residual Plot of Sealing Pressure versus the Predicted Sealing Pressure

Table 2. Effect of Different Parameters on the Sealing Pressure and Model Fit

| Parameter | Unit | P-Values |
|---|---|---|
| Fracture Width | (microns) | 0.00028 |
| Density | (lb/gal) | 0.00267 |
| D90 | (microns) | 0.05957 |
| LCM Blend | N/A | 0.11473 |
| D75 | (microns) | 0.28628 |
| Base Fluid | (WBM/OBM) | 0.30786 |
| D25 | (microns) | 0.60427 |
| D50 | (microns) | 0.75352 |
| D10 | (microns) | 0.98169 |
| **Model Fit** | | |
| $R^2$ | | 0.8 |

From the statistical analysis, it can be seen that the sealing pressure was highly dependent on the different parameters in the following order: fracture width, fluid density, D90, LCM blend/type, D75, base fluid, D25, D50, and D10. Out of these parameters, the fracture width cannot be controlled and the fluid density should be designed based the mud weight window.

### *Sealing Pressure Prediction Model*

Based on the multiple linear regression analysis, which was used to model the relationship between the different parameters and the sealing pressure, a predictive linear fit model to predict the sealing pressure was developed (Eq. 10).

$$Sealing\ Pressure\ (psi) = A_1 + Fluid_{Coeff.} + (A_2\ \rho_{Fluid}) + LCM_{Coeff.} + (A_3 \times F_w) + (A_4\ D10) + (A_5\ D25) + (A_6\ D50) + (A_7\ D75) + (A_8\ D90) \quad (10)$$

Where the constants $A_1$ through $A_8$ are as follows:

$A_1$ = - 12006.89

$A_2 = 122.4$
$A_3 = -0.9$
$A_4 = -1.85$
$A_5 = 8.93$
$A_6 = -7.28$
$A_7 = 9.69$
$A_8 = 2.45$

And $\rho_{Fluid}$ = fluid density in (lb/gal), $F_w$ = fracture width in (microns), D10, D25, D50, D75, and D90 are the particle size distribution in (microns). The other coefficient for the type of fluid and the LCM blend are tabulated in **Table 4** below.

Table 3. Empirical Coefficients for the Fluid Type and the Different LCM Blends

| Fluid Coefficient | |
|---|---|
| OBM | -87.5 |
| WBM | 87.5 |
| **LCM Blends Coefficient** | |
| CF # 1 | 2881.496 |
| G # 1 | 2995.117 |
| G, SCC, & CF # 1 | 4251.583 |
| NS # 1 | -3153.86 |
| SCC # 3 | 2418.024 |
| G & SCC # 1 | 3207.762 |
| G & SCC # 3 | 1298.886 |
| G & SCC # 4 | 5353.874 |
| G & SCC # 5 | 364.3878 |
| G & SCC # 6 | -1011.73 |
| G & SCC # 7 | -6158.57 |
| G & SCC # 8 | -4532.94 |
| G & SCC # 9 | -5785.11 |

## Conclusions

- A better understanding of the reasons behind the variation in LCM performance by means of experimental results and statistical methods was achieved.
- The statistical analysis showed that the sealing pressure is highly dependent on the fracture width, fluid density, and PSD.
- Parameters with the most significant influence on sealing pressure are fracture width, fluid density, D90, LCM blend/type, D75, base fluid, D25, D50, and D10 respectively.
- A predictive linear fit model, which could be used as a useful tool to design LCM treatment prior to field application, was developed using the parameters with significant influence on sealing pressure.
- The developed model correlated well with the collected data and resulted in an overall model accuracy of 80%.
- The knowledge of the dominant parameters affecting the sealing pressure will ensure designing LCM blends that are capable of sealing expected fracture widths that can maintain high differential pressures.
- Predicting the sealing pressure of LCM blends in advance will help in mitigating fluid losses as soon as they occur without further extensive laboratory evaluations.

## Acknowledgments

The authors would like to acknowledge Det Norske Oljeselskap ASA (Now Aker BP) for the financial support under research agreement # 0037709;

## Nomenclature

*NPT* = *None-productive time*
*LCM* = *Lost circulation material*
*PSD* = *Particle size distribution*
*PPA* = *Particle plugging apparatus*
*HPHT* = *High pressure high temperature*
*IPT* = *Ideal packing theory*
*WBM* = *Water-based mud*
*OBM* = *Oil-based mud*
*G* = *Graphite*
*SCC* = *Sized calcium carbonate*
*NS* = *Nut shells*
*CF* = *Cellulosic fiber*
*Conc.* = *Concentration in lb/bbl*

## References

1. Marinescu, Pavel. 2014. “Loss Circulation Challenges – Current Approach and What are the Next Solutions?”. SPE Lost Circulation Workshop, Dubai, 20-22 May.
2. Savari, S., and Whitfill, D. L. 2016. “Lost Circulation Management in Naturally Fractured Formations: Efficient Operational Strategies and Novel Solutions”. SPE-178803-MS, IADC/SPE Drilling Conference and Exhibition, Fort Worth, Texas, USA, 1-3 March.
3. Whitfill, D., and Miller, M. 2008. “Developing and Testing Lost Circulation Materials”. AADE-08-DF-HO-24, AADE Fluids Conference and Exhibition, Houston, Texas, USA, 8-9 April.
4. Kumar, A., Savari, S., and Jamison, D. et al. 2011. “Application of Fiber Laden Pill for Controlling Lost Circulation in Natural Fractures”. AADE-11 NTCE-19, AADE National Technical Conference and Exhibition, Houston, Texas, USA, 12-14 April.
5. Kumar, A., and Savari, S. 2011. “Lost Circulation Control and Wellbore Strengthening: Looking Beyond Particle Size Distribution”. AADE-11 NTCE-21, AADE National Technical Conference and Exhibition, Houston, Texas, USA, 12-14 April.
6. Hettema, M., Horsrud, P., and Taugbol, K. et al. 2007. “Development of an Innovative High-Pressure Testing Device for The Evaluation of Drilling Fluid Systems and Drilling Fluid Additives Within Fractured Permeable Zones”. OMC-2007-082, Offshore Mediterranean Conference and Exhibition, Ravenna, Italy, 28-30 March.
7. Sanders, M., Young, S., and Friedheim, J. 2008. “Development and Testing of Novel Additives for Improved Wellbore Stability and Reduced Losses”. AADE-08-DF-HO-19, AADE Fluids Conference and Exhibition, Houston, USA, 8-9 April.
8. Van Oort, E., Friedheim, J., Pierce, T., and Lee, J. 2009. “Avoiding Losses in Depleted and Weak Zones by Constantly

Strengthening Wellbores". SPE Drill Completion 26: 519-530. doi: 10.2118/125093-PA

9. Kaageson-Loe, N. M., Sanders, M. W., Growcock, F., Taugbol, K., Horsrud, P., Singelstad, A. V., and Omland, T. H. 2009. "Particulate-Based Loss-Prevention Material - The Secrets of Fracture Sealing Revealed!". SPE Drilling & Completion, Vol. 24(4), pp. 581-589.
10. Abrams, A. 1977. "Mud Design to Minimize Rock Impairment Due to Particle Invasion". Journal of Petroleum Technology. Vol. 29, pp. 586-592. http://dx.doi.org/10.2118/5713-PA
11. Andreasen, A.H.M. and Andersen, J. 1930. Kolloid Z.50: 217-228
12. Vickers, S., Cowie, M., Jones, T., and Tywnam, A.J. 2006. "A New Methodology that Surpasses Current Bridging Theories to Efficiently Seal a Varied Pore Throat Distribution as Found in Natural Reservoir Formations". AADE-006-DF-HO-16, AADE Fluids Conference and Exhibition, Houston, Texas, USA, 11-12 April.
13. Jahn, F., Cook, M., and Graham, M. 2008. "Hydrocarbon Exploration & Production", 2nd Edition. Elsevier Science, Oxford, UK.
14. Rehm, B., Haghshenas, A., Paknejad A. S., Al-Yami, A., and Hughes, J., 2012. "Underbalanced Drilling: Limits and Extremes". Gulf Publishing Company, Houston, TX.
15. The Drilling Manual, Fifth Edition, 2015. CRC Press, Boca Raton, FL.
16. Alsaba, M. 2015. "Investigation of Lost Circulation Materials Impact on Fracture Gradient". PhD dissertation, Department of Geological Sciences and Engineering, Missouri University of Science and Technology.
17. Sall, J. 1990. "Leverage Plots for General Linear Hypotheses". The American Statistician, Vol. 44 (4), pp. 308-315.
18. Montgomery, D. 2001. "Design and Analysis of Experiments", 5th Edition. John Wiley & Sons, Inc., New York, NY.